

A DNA origami-based device for investigating DNA bending proteins by transmission electron microscopy

Ashwin Karthick Natarajan†, Joonas Ryssy‡ and Anton Kuzyk**

Department of Neuroscience and Biomedical Engineering, Aalto University School of Science, P.O.
Box 12200, FI-00076 Aalto, Finland.

† Present address: Max-Delbrück-Center for Molecular Medicine in the Helmholtz Association,
Structural Biology, Robert-Rössle-Straße 10, Berlin, Germany.

‡ Present address: Department of Chemistry, KTH Royal Institute of Technology, Teknikringen 30,
10044 Stockholm, Sweden.

* Corresponding authors E-mail: ashwin.natarajan@aalto.fi, anton.kuzyk@aalto.fi

Supplementary Information

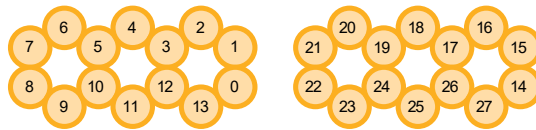
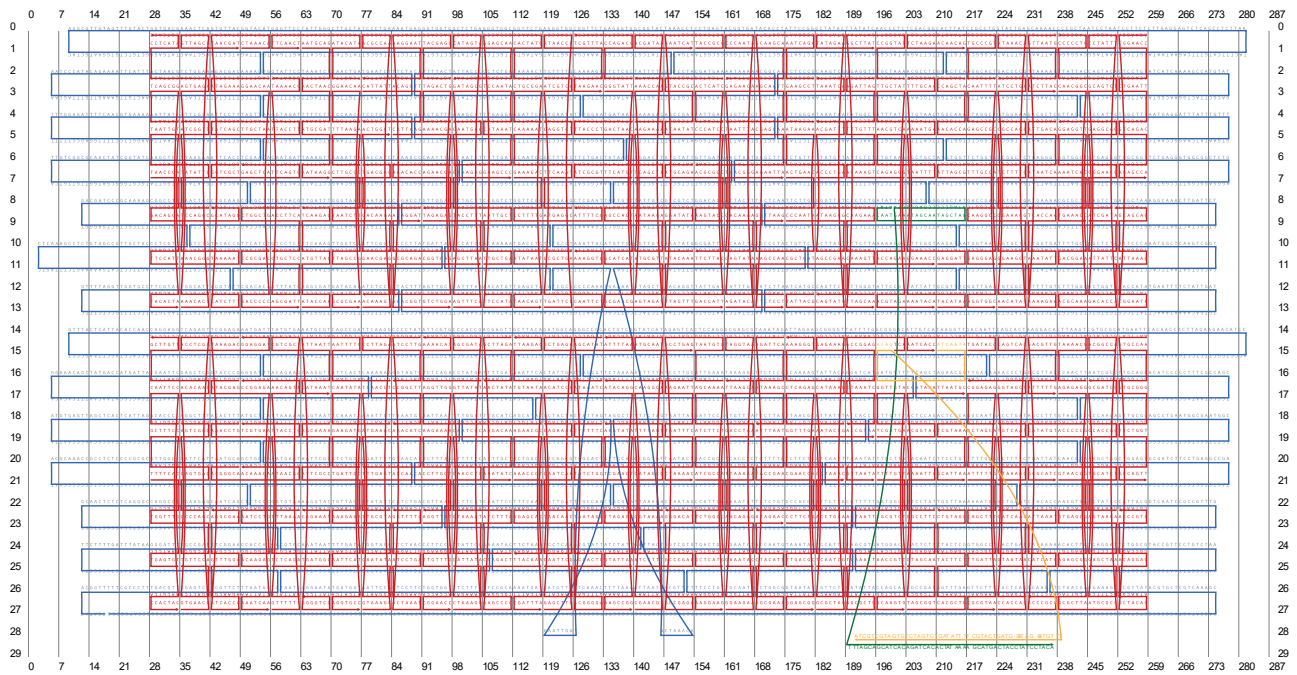


Figure S1. caDNAno design and illustration of the DNA origami template with design 1 bridge construction. Two individual strands form the bridge by hybridizing with each other and into origami.

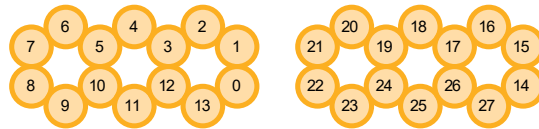
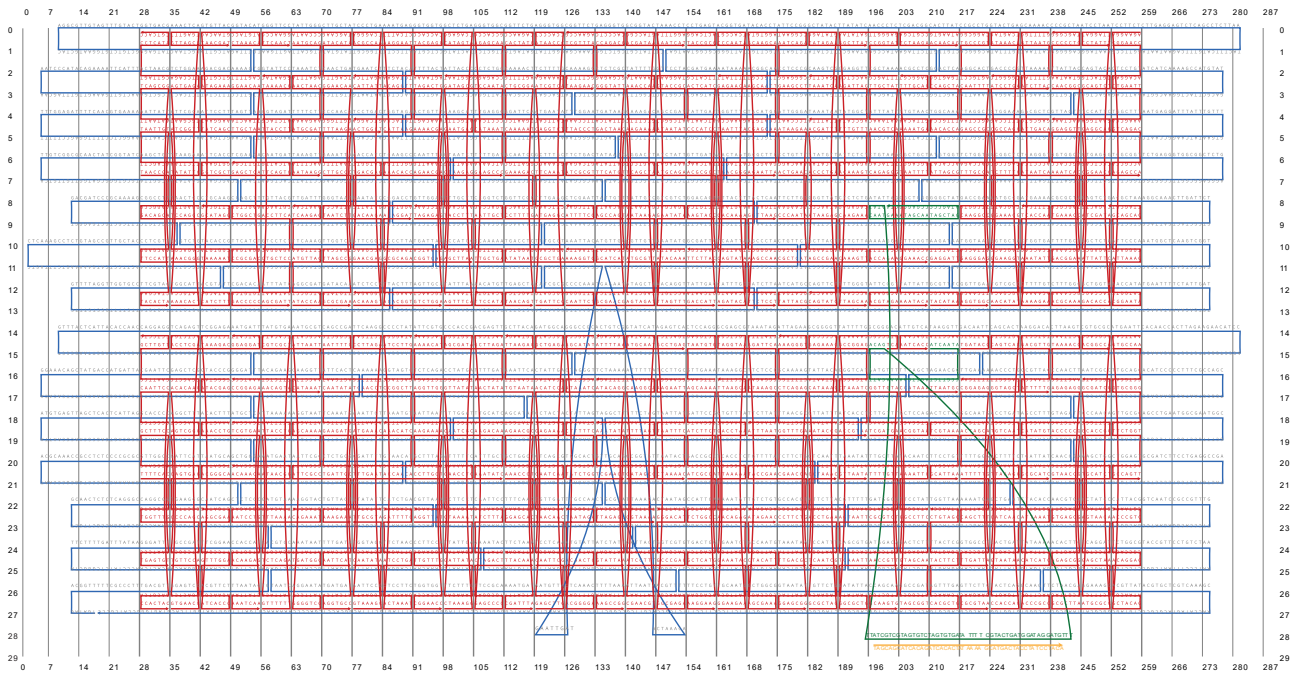


Figure S2. caDNAno design and illustration of the DNA origami template with design 2 bridge construction. A single strand forms the bridge by hybridizing to both the origami bundles and to the complementary.

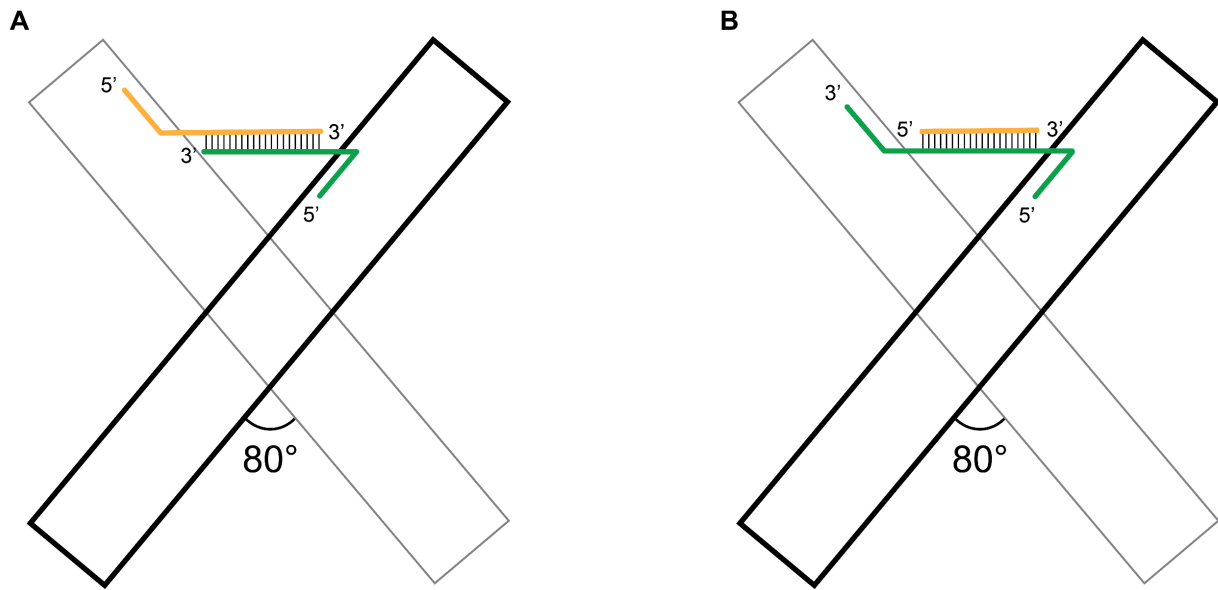


Figure S3. Illustration of the dsDNA bridge design in origami. The bridge staples have a two-nucleotide spacer and are designed to form an angle of 80° between the origami bundles. **(A)** Design 1: the bridge is formed by extensions of two individual staples from each arm; and **(B)** Design 2: the bridge is formed by a single strand hybridizing to both origami bundles and a complimentary strand.

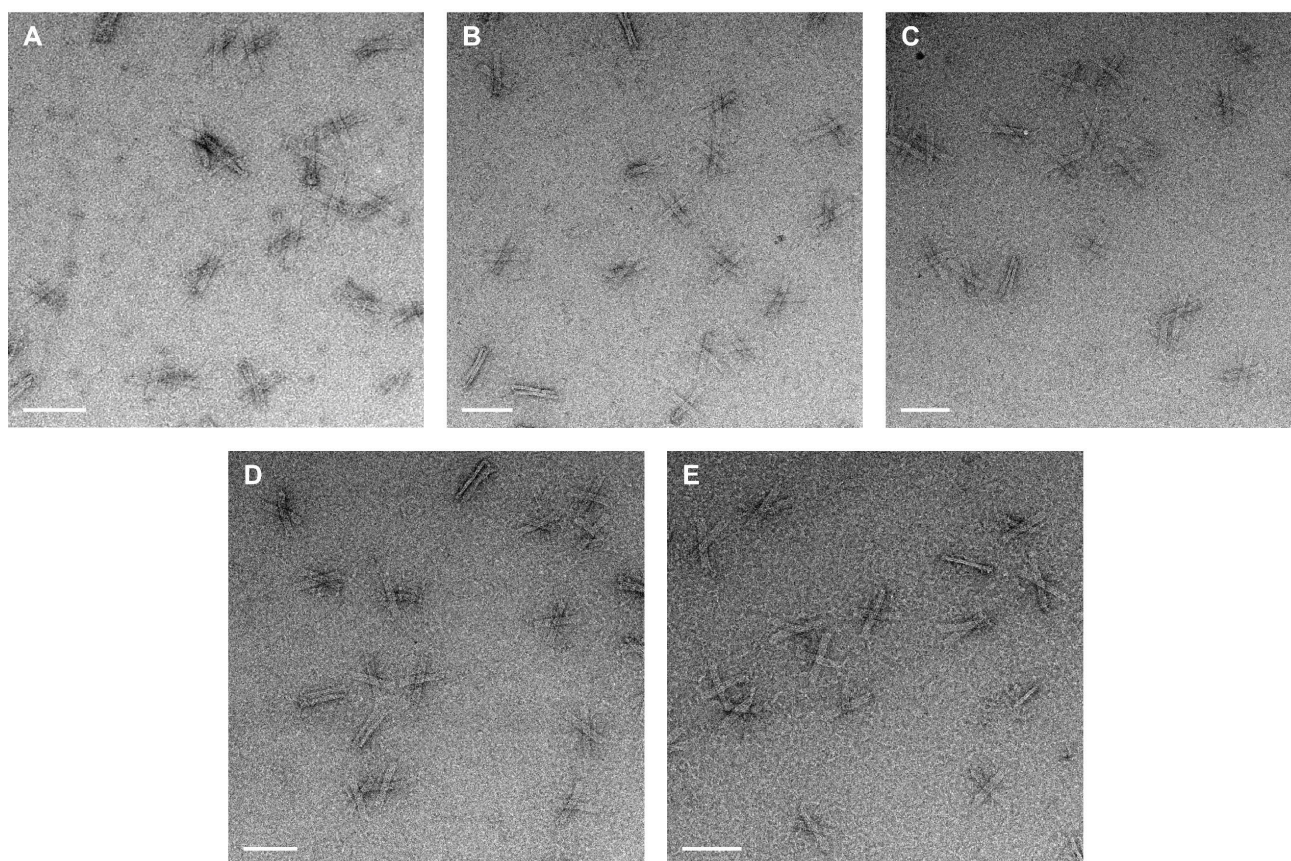


Figure S4. Micrographs of origami devices with varying concentrations of bridge staples in design 1. Devices were folded with (A) 20 nM; (B) 40 nM; (C) 60 nM; (D) 80 nM; and (E) 100 nM bridge staples concentration during annealing. Scale bars: 100 nm.

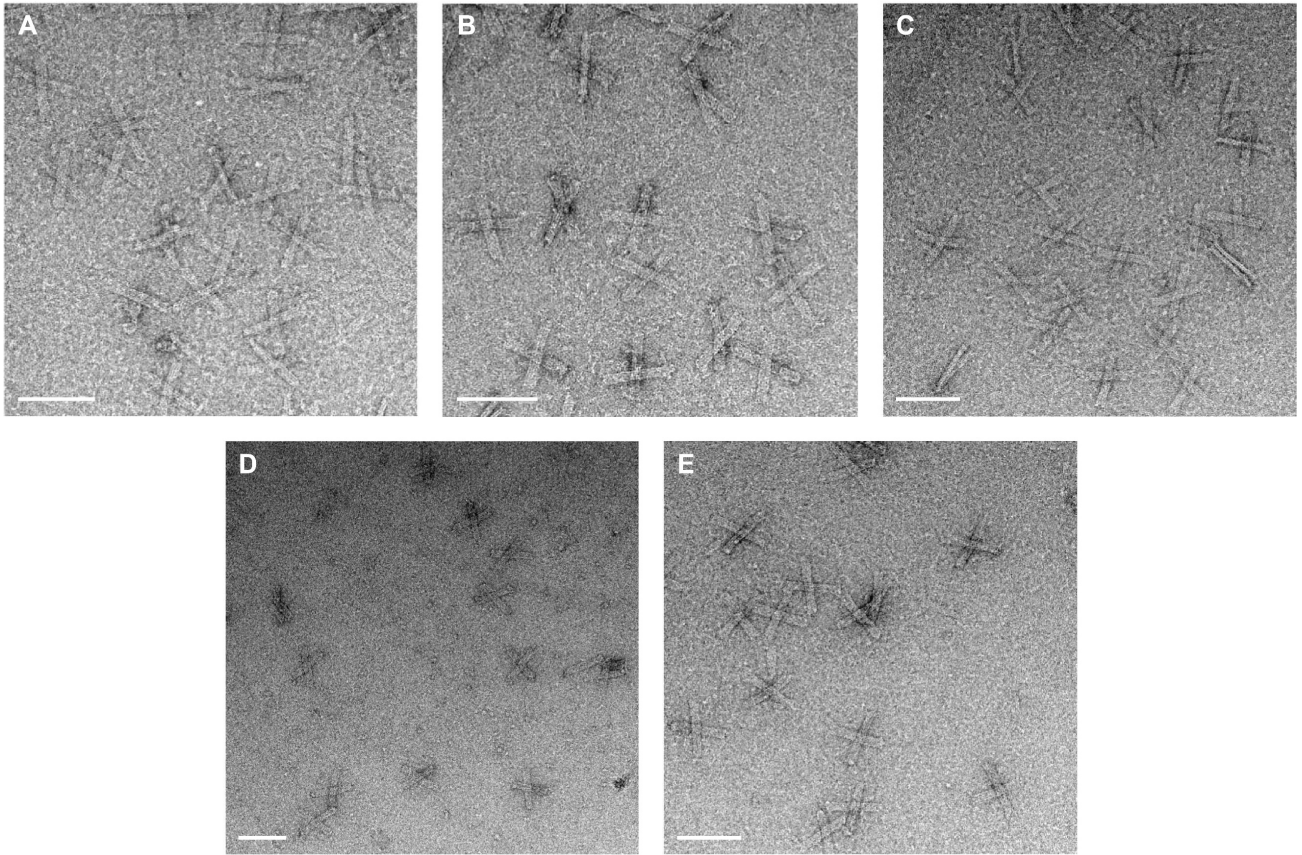


Figure S5. Micrographs of origami devices with varying concentrations of bridge staples in design 2. Devices were folded with (A) 20 nM; (B) 40 nM; (C) 60 nM; (D) 80 nM; and (E) 100 nM bridge staples concentration during annealing. Scale bars: 100 nm.

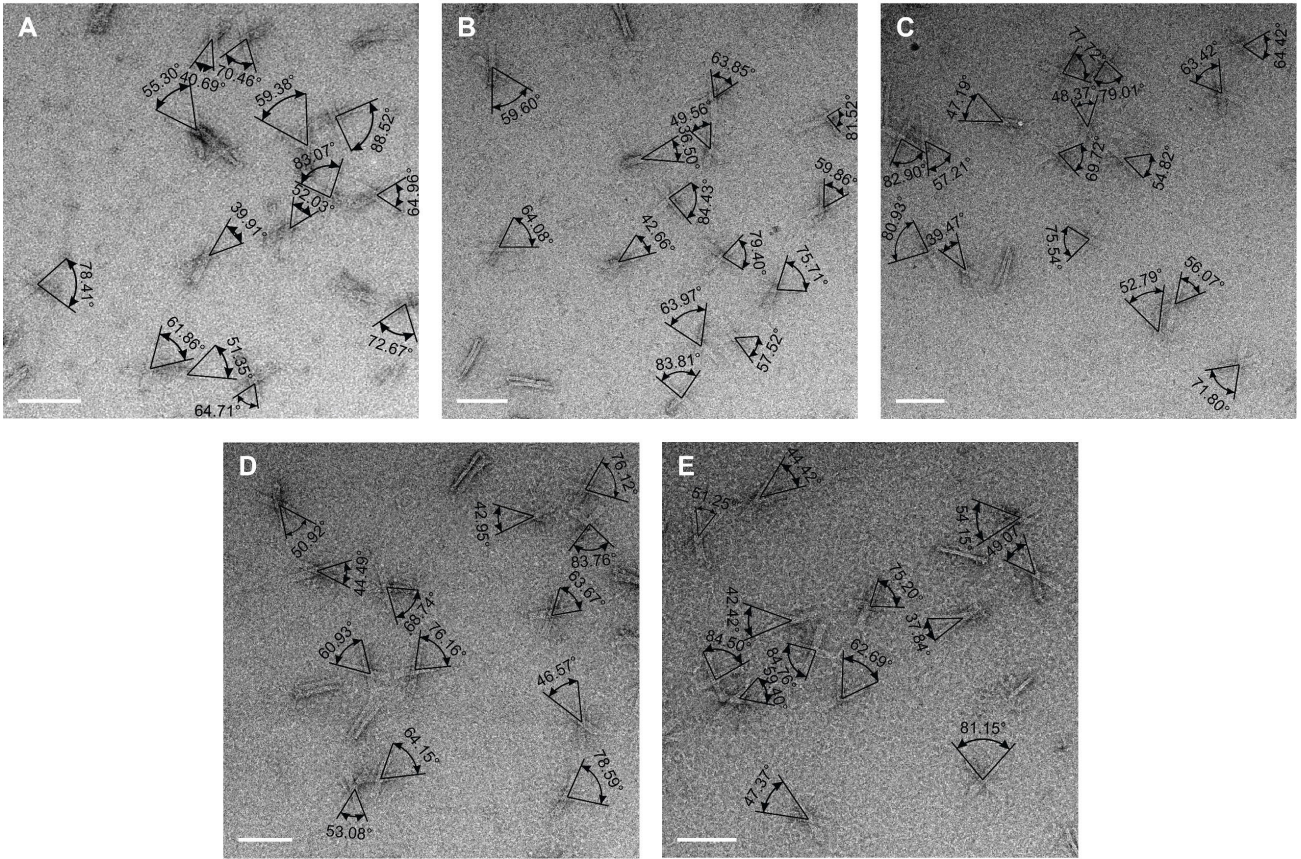


Figure S6. Angle characterization of origami devices with varying concentrations of bridge staples in design 1. Devices were folded with (A) 20 nM; (B) 40 nM; (C) 60 nM; (D) 80 nM; and (E) 100 nM bridge staples concentration during annealing. Scale bars: 100 nm.

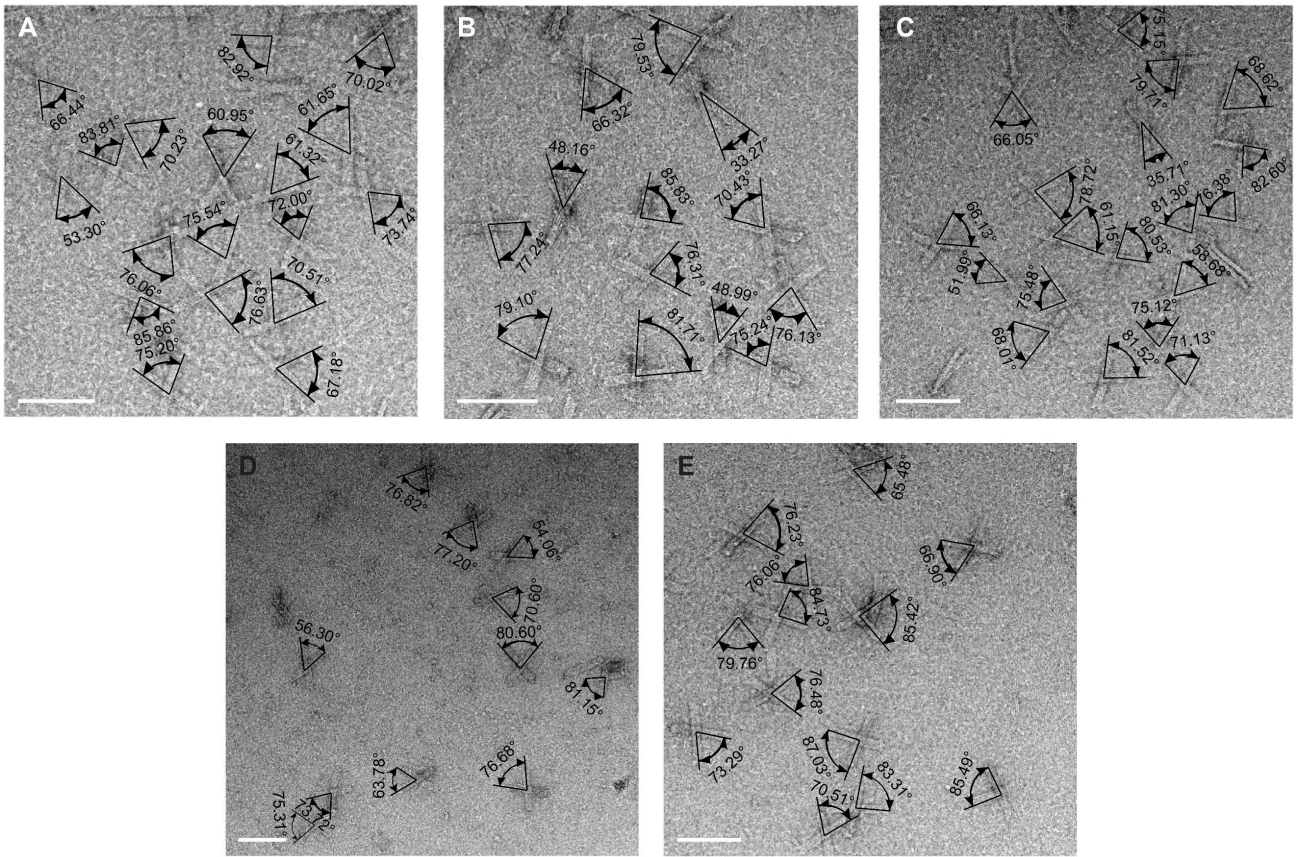


Figure S7. Angle characterization of origami devices with varying concentrations of bridge staples in design 2. Devices were folded with (A) 20 nM; (B) 40 nM; (C) 60 nM; (D) 80 nM; and (E) 100 nM bridge staples concentration during annealing. Scale bars: 100 nm.

Supplementary Note 1: Considerations for angle measurement.

The following considerations were taken while measuring the angle between the origami bundles.

- Only the acute angles were considered for angle measurement.
- If a structure exhibit bending on the grid surface such that two acute angles are not similar, the smallest acute angle was taken for angle measurement (yellow circle in Figure S8).
- If the bundles of the device overlap on top, the angle was measured only if the bundles were visibly forming an angle (orange circle in Figure S8). Hence, the number of devices forming less than 20° was small in the dataset.
- If the structure lands parallel on the TEM grid, they were not considered for measurement (red circles in Figure S8).
- The devices that are not completely visible, e.g., half structures found on the edge of the image and overlapping devices where the bundles cannot be differentiated (blue circles in Figure S8) were not considered for angle measurement.

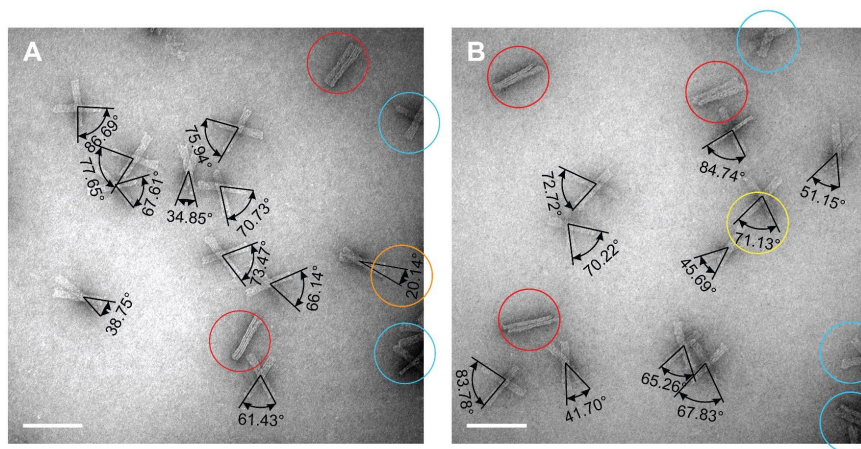


Figure S8: Representative origami devices not considered for angle measurements. The circles (A) and (B) represent the devices not picked during angle measurements. Refer to Note S1 for information on the circles. Scale bars and diameter of circle: 100 nm.

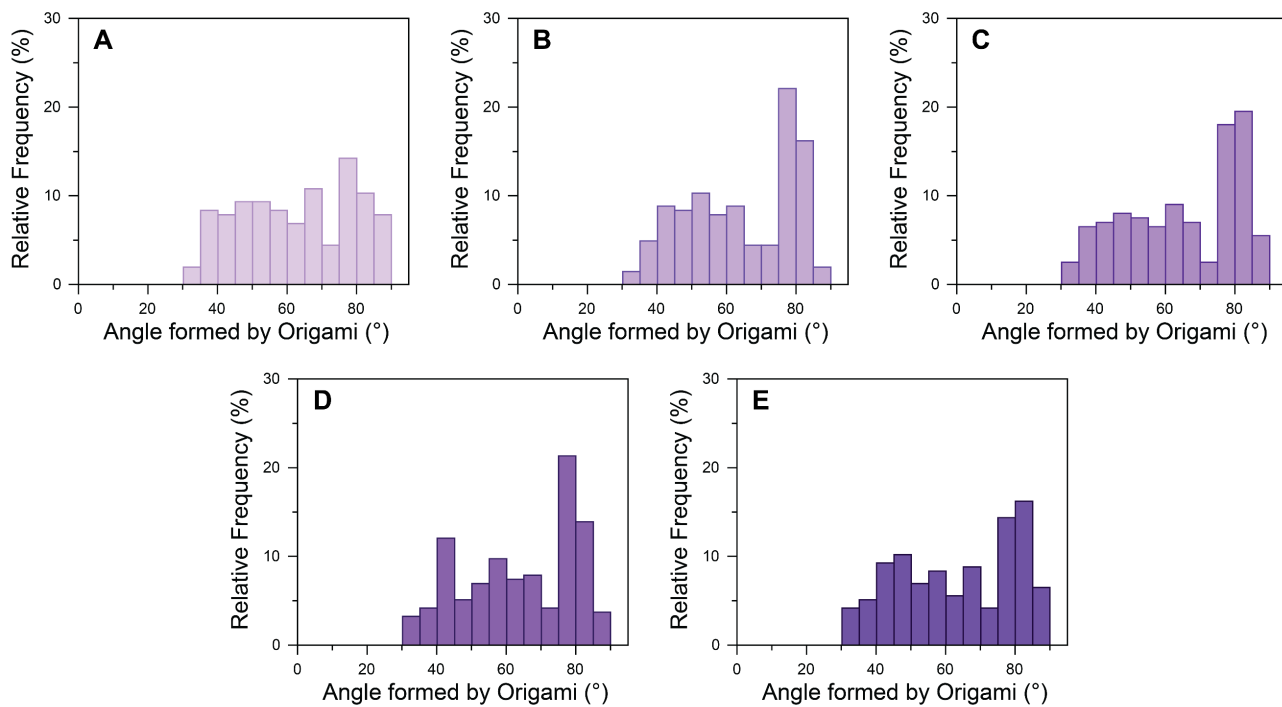


Figure S9. Histogram of the acute angle between two bundles of DNA origami-based device for structures folded with varying concentrations of bridge staples in design 1. Devices were folded with (A) 20 nM; (B) 40 nM; (C) 60 nM; (D) 80 nM; and (E) 100 nM bridge staples concentration during annealing.

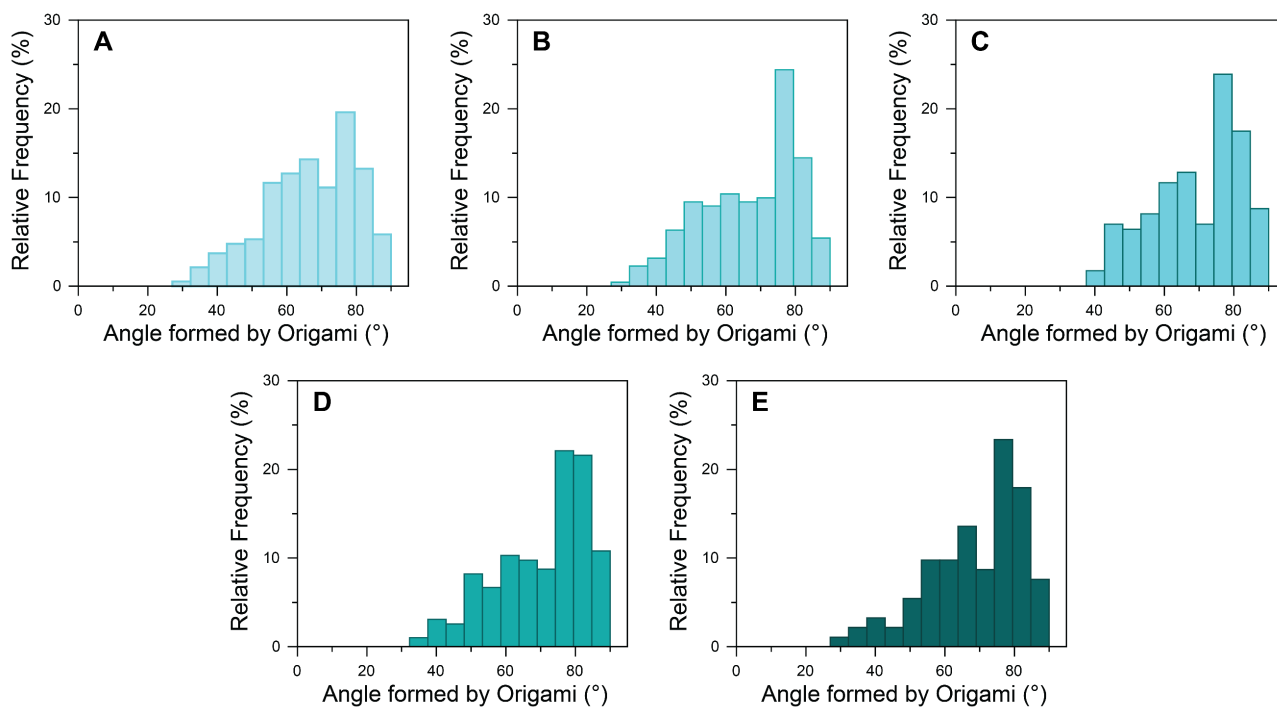


Figure S10. Histogram of the acute angle between two bundles of DNA origami-based device for structures folded with varying concentrations of bridge staple in design 2. Devices were folded with (A) 20 nM; (B) 40 nM; (C) 60 nM; (D) 80 nM and (E) 100 nM bridge staples concentration during annealing.

We hypothesized that when the bridging staple concentration was high (10-fold excess) in design 1, the individual staples hybridized to the scaffold in prescribed regions can find their complementary strand from the solution rather than the other staple strand, thereby forming structures without a defined angle. Whereas in design 2, while the highest yield was at 8-fold molar excess of bridging staples, the overall yield was relatively close in other experiments as well (~37% for 4-fold excess, ~39% for 6-fold excess, and ~39% for 10-fold excess), implying little dependency on the bridging staple concentration.

Supplementary Note 2: Angle calculation

Upon addition of Human TBP to the origami structure, the TATA box bends $\sim 90^{\circ 1-3}$ decreasing the end-to-end distance of the bridge (AD- R_b) thereby bringing the origami bundles closer and changing the angle between the bundles. The change in angle was observed using a TEM. The geometry of the bridge and subsequent change in angle are presented in Figure S11. The end-to-end distance of the bridge between the origami bundles (R_b) can be calculated from the angle between the bundles using equation 1.

$$R_b = 2R \cdot \sin\left(\frac{\varphi_b}{2}\right) - 2r \cdot \cos\left(\frac{\varphi_b}{2}\right), \quad \rightarrow \quad \text{Eq. 1}$$

where R_b is the distance between the central pivot and the bridging staple, r is half the width of the origami bundle and φ_b is the angle between the origami bundles after TATA box is bent.

The bend angle of the TATA box upon TBP binding changes the end-to-end distance R_b which can be calculated as follows:

If A is considered the point of origin (0,0) then the co-ordinates of D are calculated by

$$x = L_1 \cos\theta + L_2 + L_3 \cos\theta, \quad \rightarrow \quad \text{Eq.2}$$

$$y = L_1 \sin\theta - L_3 \sin\theta, \quad \rightarrow \quad \text{Eq.3}$$

where θ is $\alpha/2$ and α is the bend angle of the TATA box upon TBP binding. If DNA was considered as a beam entering and exiting a prism, then the overall bend angle (α) can be defined as the angle between the incoming and outgoing DNA helix. Then, the distance AD can be calculated as

$$R_b = \sqrt{x^2 + y^2} \quad \rightarrow \quad \text{Eq.4}$$

Since the end-to-end distances relate to α and θ , the value of TATA box bend angle α can be calculated from the angle between the origami bundles θ . The value of α was calculated by solving the equations in Matlab.

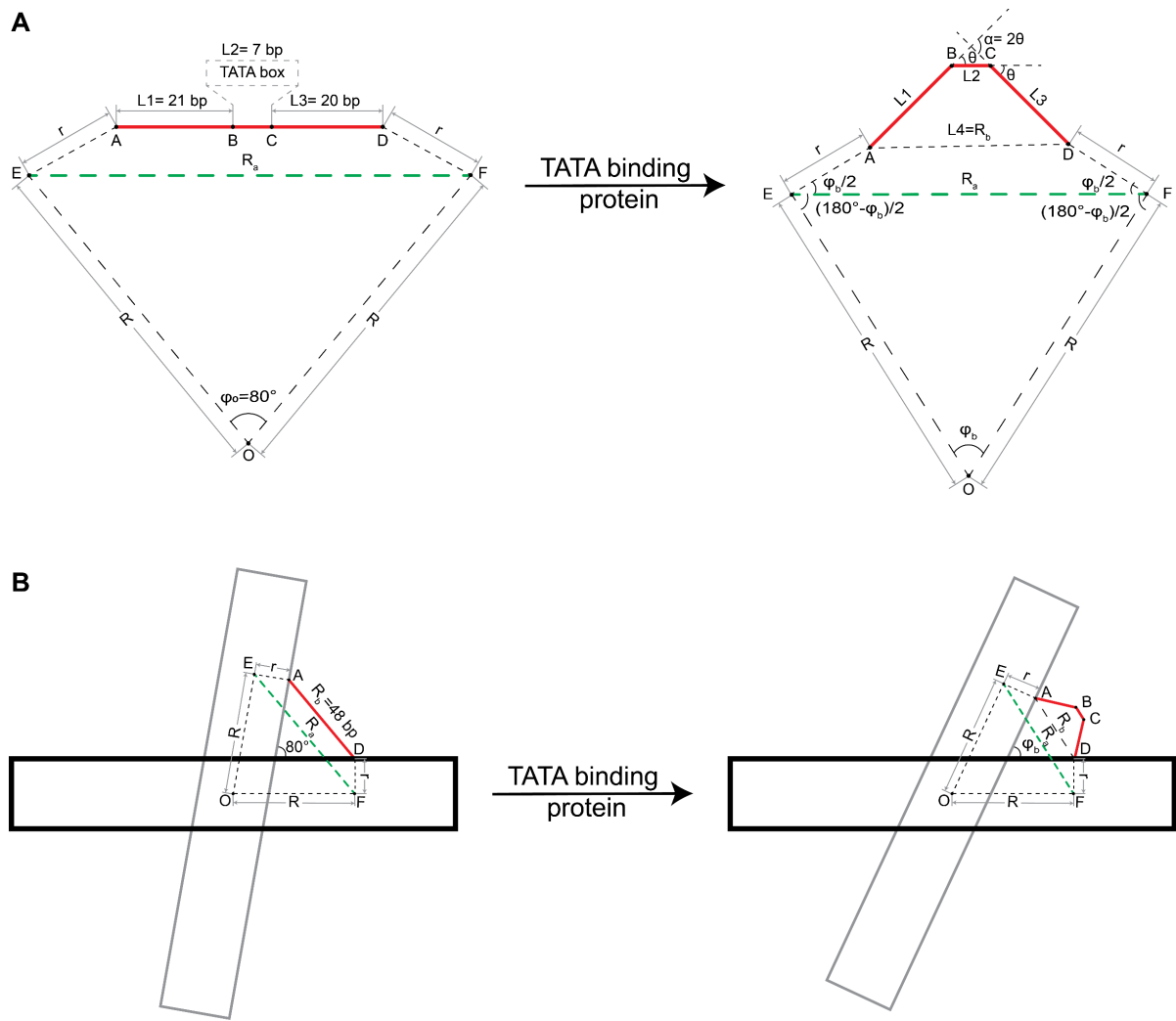


Figure S11. Scheme of TBP binding to TATA box and subsequent bending. The change of angle reduces the end-to-end distance thereby bringing the origami bundles closer together. **(A)** Representation of TATA box bending by TBP where $R=64$ bps (~ 21 nm) and $r \sim 7.5$ nm; **(B)** Representation of the change in angle between the origami bundles caused by bending of TATA box by TBP and **(C)** Two-kink model of TATA box bending.

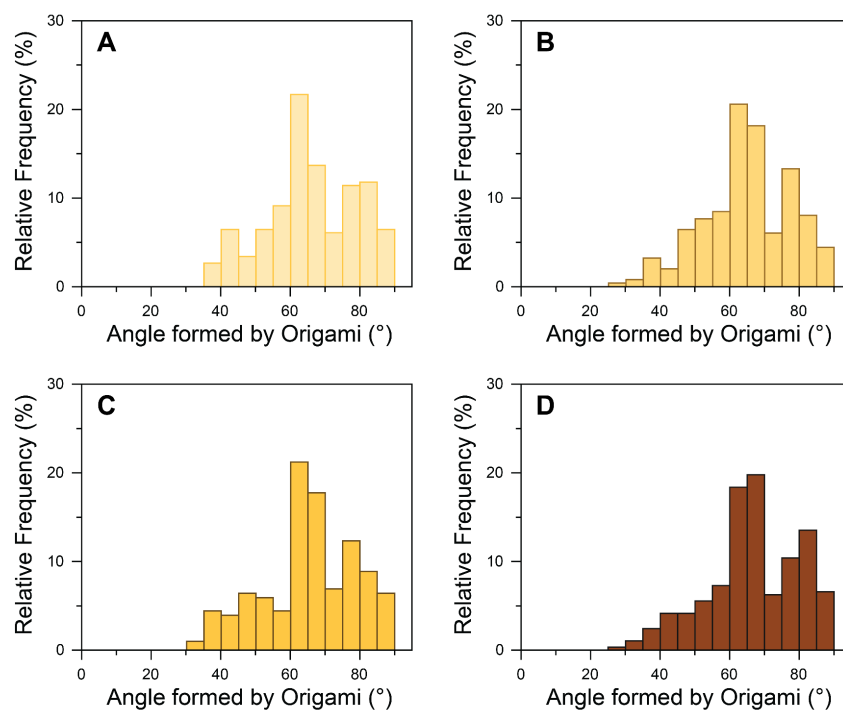


Figure S12. Histogram of the acute angle between two bundles of DNA origami-based device with consensus S1 sequence in design 1 incubated with TBP. The concentration of TBP was **(A)** 25 nM TBP; **(B)** 50 nM TBP; **(C)** 100 nM TBP and **(D)** 150 nM TBP. There was no significant change between the angle distribution of origami incubated with 100 nM and 150 nM of TBP.

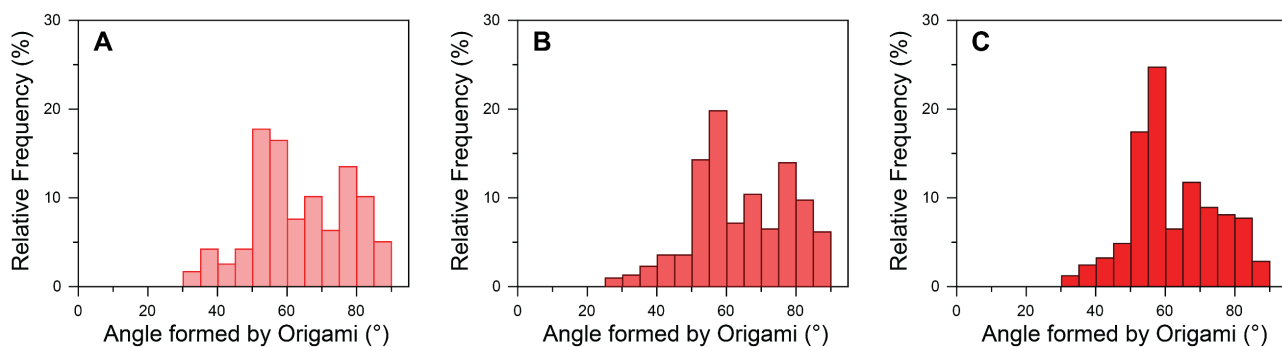


Figure S13. Histogram of the acute angle between two bundles of DNA origami-based device with consensus S1 sequence in design 1 incubated with TBP and TFIIA. The concentrations of TBP and TFIIA were **(A)** 25 nM TBP and 25 nM TFIIA; **(B)** 50 nM TBP and 50 nM TFIIA and **(C)** 100 nM TBP and 100 nM TFIIA. The distributions have an observable emergence of peak around 55° angle formed by origami.

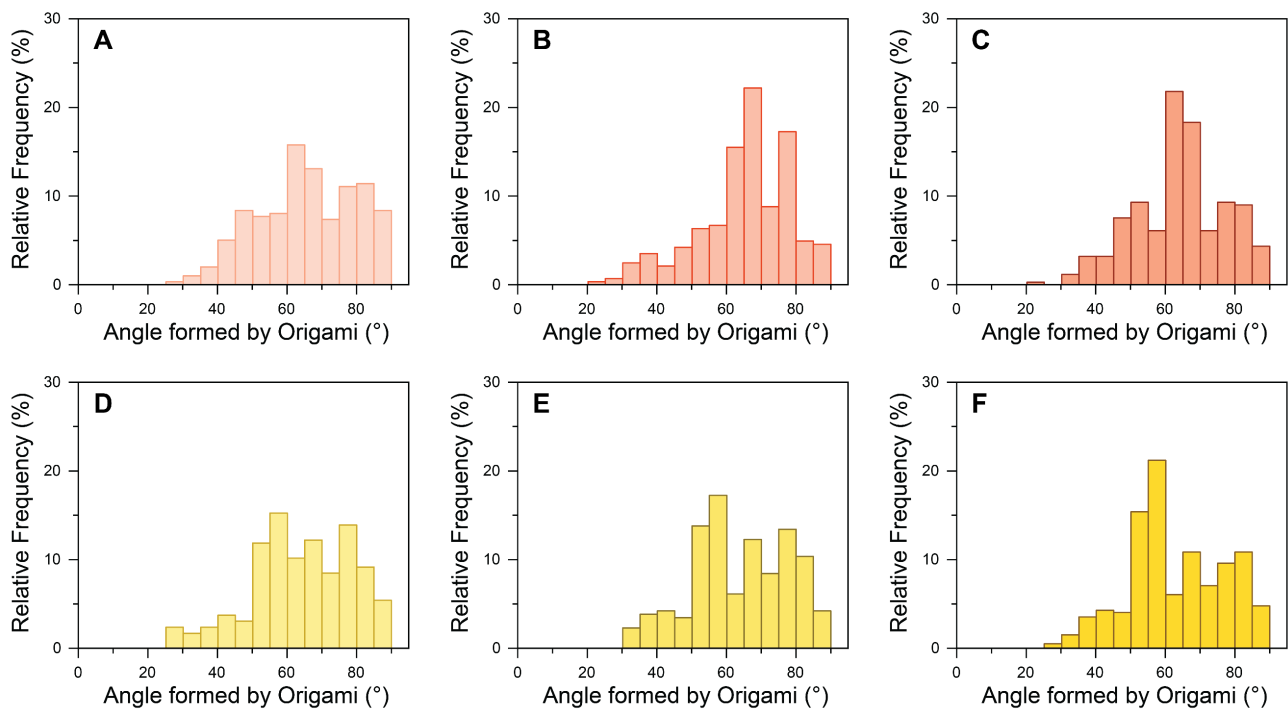


Figure S14. Histogram of the acute angle between two bundles of DNA origami-based device with S1 sequence incubated with TBP, TFIIA and TFIIB. The concentration of TBP, TFIIA and TFIIB were **(A)** 25 nM TBP and 25 nM TFIIB; **(B)** 50 nM TBP and 50 nM TFIIB; **(C)** 100 nM TBP and 100 nM TFIIB; **(D)** 25 nM TBP, 25 nM TFIIA and 25 nM TFIIB; **(E)** 50 nM TBP, 50 nM TFIIA and 50 nM TFIIB and **(F)** 100 nM TBP, 100 nM TFIIA and 100 nM TFIIB.

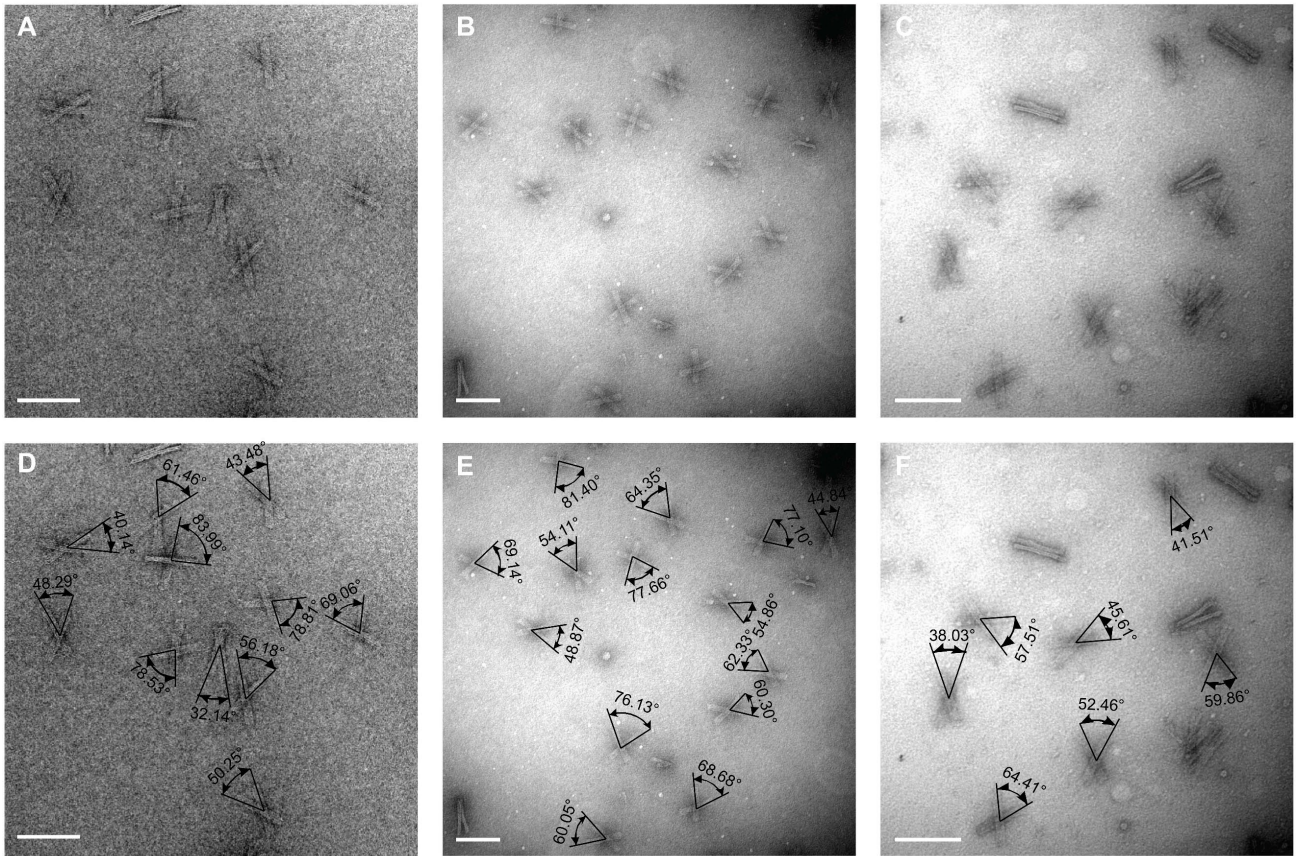


Figure S15. Micrographs of origami devices with S2 sequence in design 1 and their corresponding micrographs with measured angles. The micrographs represent **(A)** Control devices with S2 sequence forming 80° between the bundles; **(B)** Devices incubated with 100 nM TBP and **(C)** structures incubated with 100 nM TBP and 100 nM TFIIA. Scale bars: 100 nm.

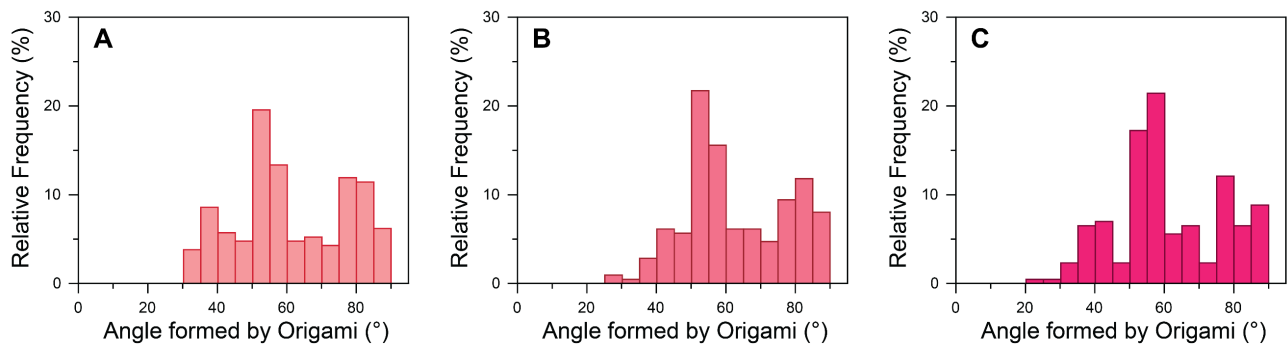


Figure S16. Histogram of the acute angle between two bundles of DNA origami-based device with S2 sequence in design 1 incubated with TBP and TFIIA. The concentration of TBP and TFIIA were (A) 25 nM TBP and 25 nM TFIIA; (B) 50 nM TBP and 50 nM TFIIA and (C) 100 nM TBP and 100 nM TFIIA. The distribution has an observable peak around 55° angle formed by origami. The results were similar to that of the consensus sequence indicating that these bases do not alter the extent to which the TATA box is bent by TBP.

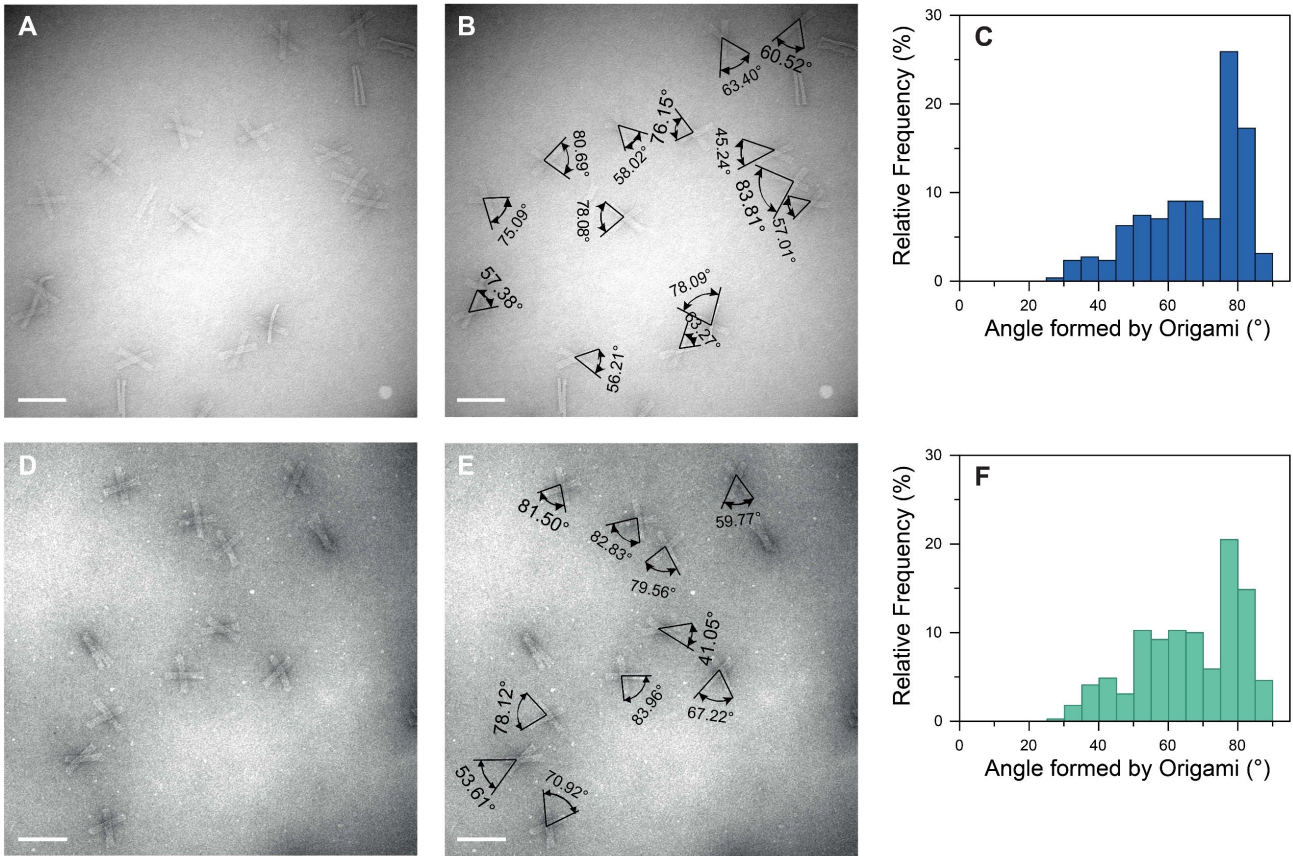


Figure S17. Control experiments of 80° forming origami with S1 sequence in design 1 incubated with TFIIA and TFIIB. The micrographs and their corresponding angle measurements for devices incubated with 50 nM TFIIA (**A, B**) and 50 nM TFIIB (**D, E**). Histogram of the acute angle between two bundles of DNA origami-based device incubated with (**C**) 50 nM TFIIA and (**F**) 50 nM TFIIB. Scale bars: 100 nm.

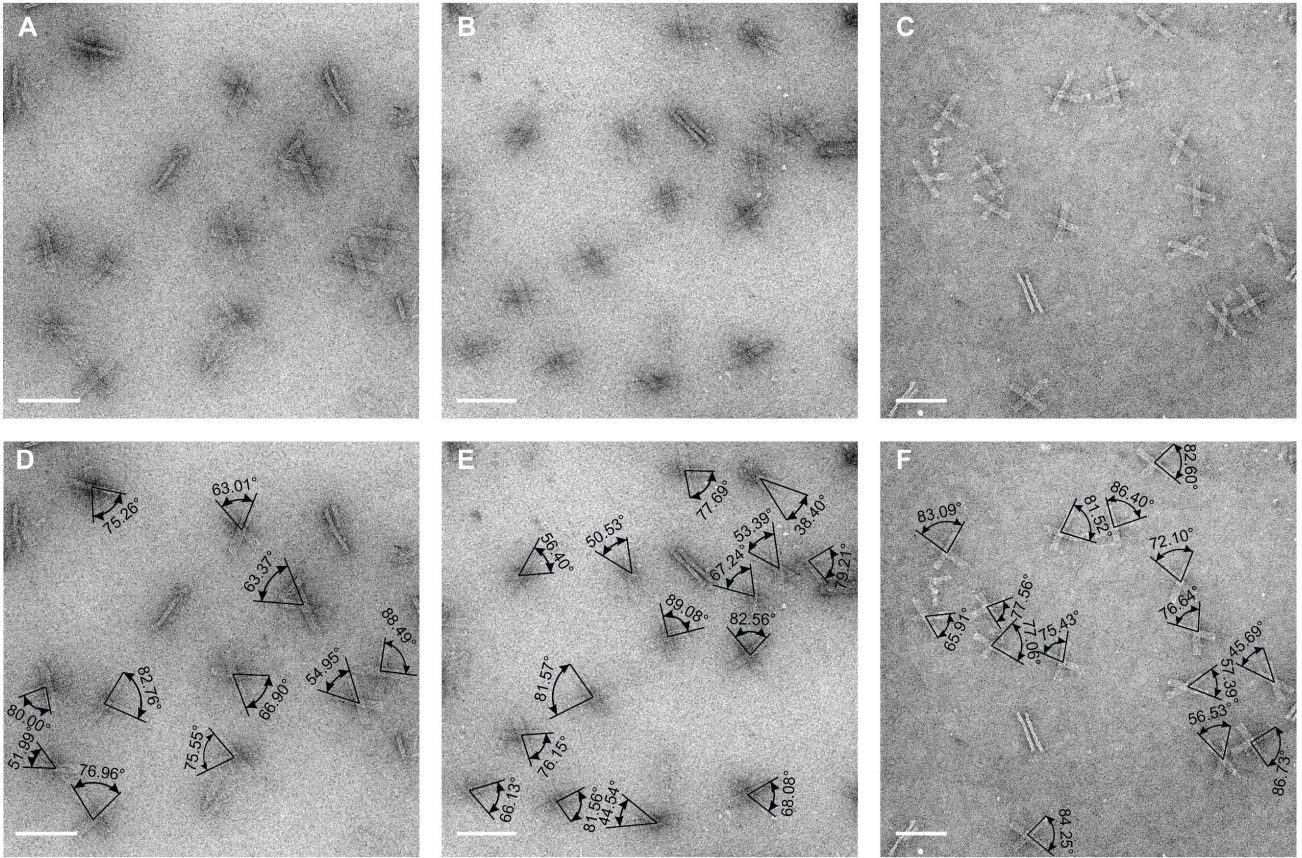


Figure S18. Micrographs of origami devices with scramble S3 sequence in design 1 bridge and their corresponding angle measurements. The micrographs and their corresponding angle measurements are represented in **(A, D)** Control devices with a bridge forming 80° between the bundles; **(B, E)** devices incubated with 50 nM TBP and **(C, F)** devices incubated with 50 nM TBP and 50 nM TFIIA respectively. Scale bars: 100 nm.

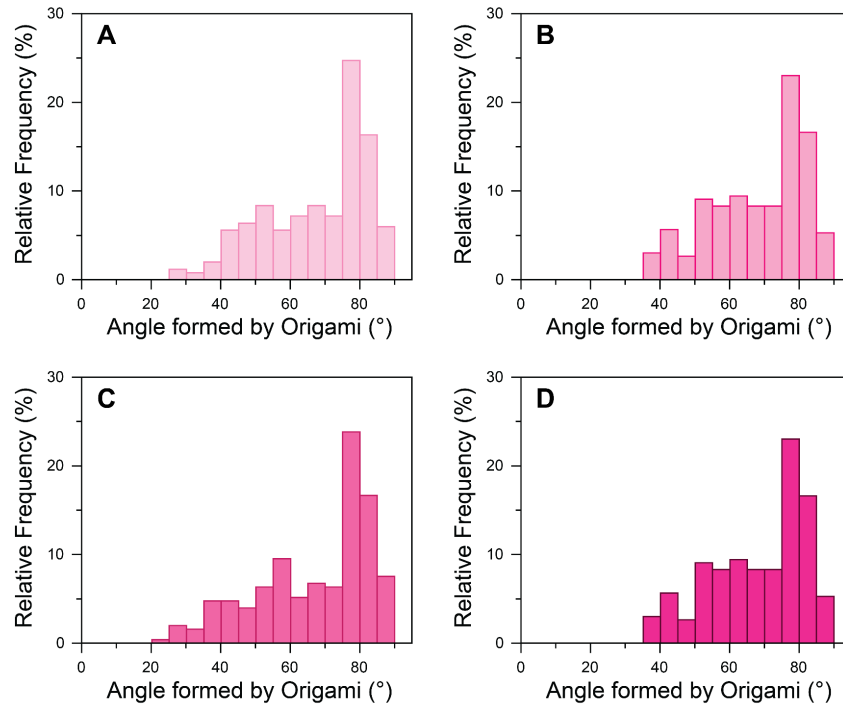


Figure S19. Histogram of the acute angle between two bundles of DNA origami-based device with scramble S3 sequence in design 1. The histograms represent **(A)** control devices; Sample incubated with **(B)** 50 nM TBP; **(C)** 50 nM TBP and 50 nM TFIIA and **(D)** 50 nM TBP and 50 nM TFIIB. There was no change in distribution compared to control, implying that the TATA box is required for the bending by TBP.

Supplementary Table S1: Staple sequences for the DNA origami template.

Start	End	Sequence	Length	Name
4[34]	13[34]	AATAATTCAGCGGCTACGAATACACTA	28	core1
8[90]	6[77]	AGGTCCGGATATTCTGACGAGGATGGTT	28	core2
24[146]	18[133]	AGTAATCTTTTAGTCTAGAAAAAGCCTA	28	core3
25[161]	16[161]	GAAATACCATTGCATTAAGCAGCCTTA	28	core4
26[146]	16[133]	TATTAATCAAGGCATAAAAAATTTTAGA	28	core5
16[104]	14[91]	TCATAGGTCTGAGAAAAACATCACGAAT	28	core6
22[146]	23[146]	TCTTTAATGCGCAGTTAGAGCCGTA AAA	28	core7
25[203]	17[216]	GTAGCAAATCGGCCCATAAATTAATGC	28	core8
18[34]	27[34]	GGGGTGCCAATCCAACGTCACCACTAC	28	core9
13[35]	1[48]	AAACTTGTAGTTTGTAGCGTAACGAT	28	core10
4[223]	13[223]	AGCCTAACAAATTTTTCAACCAGGTGGC	28	core11
25[245]	16[245]	GAGCTAAGCTTTCCGCGATCGGGCGATT	28	core12
2[139]	0[126]	GCGAGAGCCAGACGCACCCTCAGAACCG	28	core13
26[62]	16[49]	GATTACAAACAGTACTTCTGTAAATCCC	28	core14
4[76]	13[76]	CGTTGGGGGAACAATTGTATCGCGCGAA	28	core15
4[118]	13[118]	TGAATCCCTGCGGATAGCTCATAACAGT	28	core16
26[230]	16[217]	CTGAGTAGGTAGCTCAGGGTTTTTCAA	28	core17
23[203]	18[203]	GGCCTTCAAGAGTCACGGTAACTGGAGC	28	core18
27[140]	15[153]	CGAACGTATGATACATGCAATGCCTGAG	28	core19
9[245]	4[238]	ATCGATATAGAGCCGAGGCAGGAATGGAACTAAC	35	core20
2[202]	13[195]	TTTAGCGCCGGTATGAGGGTTGATATAATTAGCAA	35	core21
12[174]	12[182]	TAAGATCAAGCCAACGCTCATAGCCGAAAGAACTG	35	core22
27[98]	16[105]	CTAAAGGCGGTGGGAGCGATAGCTTAGAATCAAAA	35	core23
25[140]	22[147]	ATCCTTTGCCCGACCACGACCGGGACATCTATTAG	35	core24
1[49]	12[42]	CTAAACAATGTACCGTAACACCATCTTTAATACGT	35	core25
23[175]	19[195]	CCTTCTGACCTGAAAAATGGAAATACCGACCGTAA	35	core26
18[132]	21[139]	CTAATAGCTTTTTCAGTGCCATATCTGGTCAACT	35	core27
6[97]	8[91]	TAAATTGGGCTTGAAAAACCCAGAACGACTCCAAC	35	core28
27[77]	16[84]	GTAAAGCCCTTGAACTTAGAATCCTTGACTACC	35	core29
5[84]	9[90]	CATTAAGAAAACGATTAATCATAAGGGAACAGGAT	35	core30
4[202]	13[209]	AATAAACTTGCTATACGGAATACGTAGAAAATACA	35	core31
22[83]	22[91]	AATATACTTTGAATACCAACACCTTGCTTTAACG	35	core32
19[196]	23[202]	TCGATGATGTCCATCACGCTGAGTAATTCGCGTCT	35	core33
2[181]	13[174]	CGGGAGGAATCAGACCGGAATAGGTGTATTCTCCT	35	core34
6[153]	9[160]	AATAGATATGCAGAACGCGCCTCTGTCCAAGTACC	35	core35
25[77]	18[84]	CAATATACGGAATTTGAACCTCCGGCTTACATTA	35	core36
21[196]	21[188]	TTTTGTTCGCCATCAAAAACGTAAGAATCCTAAAC	35	core37
1[154]	13[160]	TACCGCGACTCAGGAGGTTTATTAGTTTGACCATT	35	core38
22[209]	21[195]	ATAGGAAAAAATTCGATTGTATAAGCAAATATTTAGTTAATA	42	core39
7[175]	7[174]	ACTGAACACAAGAATTGAGTAAAGTAATTGACGGGAGAATTA	42	core40
19[168]	22[168]	ATTTAATTAACATACCGAACGAACCAACGTGGCACAGACA	42	core41
24[111]	20[98]	GTATTCATCTTTAGGAATTGAGGAAGGGAACCTCGAAAAAT	42	core42

27[56]	17[69]	GTTTTTTTCACATACGTCGCTATTAATTAACCTGCATAAAT	42	core43
4[139]	11[139]	CTTATCATTCCAAATTACCCTGACTAACCCAACATGCATCAT	42	core44
22[251]	21[237]	GGATAGGTGCATCTCCAGCTTTCGGTTGATAATCAGCGCATC	42	core45
7[140]	7[139]	TCAGCTAAAGTCTTGATTATAGTCAGAAATCGCGTTTCATGT	42	core46
23[77]	20[77]	TTGCGTACCTACCAATGAAACAAACATCATGTTACAAAATCG	42	core47
22[62]	22[63]	TTACATCGGGAGAGAATCCTGTTTAAAACAGAAATGTACCTT	42	core48
12[195]	8[182]	ACCCAAACAAAGTTTAAAGAAAACAAGAAACAGAGAGATAACCC	42	core49
3[238]	1[251]	CAACGGCGCCAAAGACGCAAAGACACCATTAGGATCCTATTT	42	core50
4[160]	11[160]	ATCAATAAECTCATCGTCAATAAECTGTTATACAAATTCCTAC	42	core51
16[160]	26[147]	TTTCAACTAATGTGCCTGGAGTGACTCTGGCGAGAAAAACGT	42	core52
20[48]	20[49]	TGCATTAACGGGCAACAAACAATAACGGATTCATTTCCAGC	42	core53
11[35]	4[35]	AAACGGGTAAAAATCGGTGTACAGACGGATCGGTTTGCGAAT	42	core54
17[238]	15[251]	AGAGAGGTCGTTAGGCGCTTAATGCGCCGCGCACGACGGCCA	42	core55
6[48]	6[49]	GGTGAATGGTCGCTGAGCTCATTCAGTGATCATTTGTTCGA	42	core56
7[28]	8[42]	TAACCGAAAGGCCGGACAGCATCCAGGCGCATAGGCTTGCAG	42	core57
16[153]	21[153]	GCAAGGAAAGAATTATAATTATAATTCAGTATTACTAAAAC	42	core58
10[153]	9[139]	CATATTTGAATATAAGACGACGACAATAAAACAATAAGCCAGT	42	core59
13[119]	3[132]	TGATTCCCCACCTATAACCCTCGTTTAGCTTTTGTAGAAC	42	core60
16[244]	26[231]	AAGTTGGTAAAACGACTTAAGTGCCTTACCCGCCAACTTGC	42	core61
7[112]	8[126]	GAAAGACGCGAACCCCTTTTGATGAGGCATTTTCGATTCGAG	42	core62
27[119]	14[133]	GAGCTTGTGCCATCGCTGAGAAGCATATATTTTAACGACAGT	42	core63
25[224]	22[224]	GTAATAACATCATCTTTTATAATTAATGGTGTAGATTCAGC	42	core64
12[181]	1[195]	GCATGATTATTACGAGTATGGTATAGCTATAGAAGGCTTAT	42	core65
2[76]	1[62]	TCAGTTGATACATATAGCAAGCCCAATAGGAACCCCTCAACT	42	core66
27[35]	14[49]	GTGAACCACTTGAACCTCGATAAAGACGGAGGATAATCATT	42	core67
22[125]	24[112]	ATCAACACAATCAACGCTGAGAGCCAGCAGAACGCTTTAGAA	42	core68
6[76]	12[77]	TAATTTCTTTAAGATGACCAATTAGCCGGAACGAGCGGAGAT	42	core69
7[70]	5[83]	CTTGCCATTACCCTAATCTTGACAAGAACCGAACACTGGCT	42	core70
18[244]	25[244]	AATCTACAAAGGCTCATATGTACCCCGGAAGTGTAGAGCGG	42	core71
27[224]	17[237]	CCACCACAGTGTGCAGTCACGACGTTGGTAACGCATTTTGT	42	core72
2[97]	13[97]	AGTAAAATACGAGGCACCACCCTCATTTACACGGTGTCTGGA	42	core73
12[41]	0[28]	AATGCCAAGTGAGATTCCAGACGTTAGTCTCATACGTCACC	42	core74
13[224]	3[237]	AACATATTCAGTACATAAACAGTTAATGGTTTTAAATCTTAC	42	core75
14[174]	23[174]	CTATTTAAGCGAAACGCCAGCCTACATTCATTGGCATAGAAC	42	core76
10[125]	10[126]	AGGCAAAGAGGTCAATATAATGCGCTGAAAAGGTGGTAATTT	42	core77
2[118]	12[105]	AGTTTTGCACTATCCAGAACCGCCACCCTTCCATAACATGTT	42	core78
8[250]	11[244]	AGACTGCGGAACCCCTCAGAGCCACCGAGGTTAGCAAAGACGGAA	48	core79
3[133]	1[153]	GGGTATTATTTTCAGCGAACGAGTAGATGTACCGCACGATAAAAATCAT	49	core80
25[56]	18[49]	TCTCAGATGATGGCATTATTTGCACGTGTTACCTGTTTTAATGAGCAT	49	core81
23[91]	21[111]	AGGTTATCTAAAATTGAATAACAATCGCAAGACAAAGCAAATAAATATC	49	core82
11[105]	7[111]	TTGCTGATTTTGAATTGCTAGACCGGAAGCAAAGTAAGAGGAAGCCC	49	core83
2[195]	7[202]	AACCTCCAGATTAGACCATATTTGTTTAGAGAATACAAAGTCAGAGGG	49	core84
27[161]	18[168]	GGAAGAACGCTCGCTAGGTAAGATTACGGGAGAAAATAAGCATAAGAA	49	core85
4[237]	9[244]	GAGCGTCATTGACAACCCTCAATAATCAAAAATCACTAGCGCGTGAAACC	49	core86

21[238]	18[245]	GTAACCGTCACGTTGTGAGCGAGTAAACAATCCTGAGCACCGCTGTTGGG	49	core87
21[28]	18[35]	TTTTACCCGCCTGTGGTTTGC CCCAGCATCGGCAAGTCGGGAAAGCCT	49	core88
2[216]	11[223]	TGAGTGCCAGCTATTTGCCAAACACCAGAGCCGCATTACCAGAGGGAG	49	core89
16[83]	26[63]	TTTTTTGAGTGAATAATTTCTCGGCTGACGCATTGGGGTCGTATTCT	49	core90
27[203]	22[210]	TAGCGGTCACGCTGTCAAACCTACTTCTCGAGTAACTGTAGCTTAACCA	49	core91
15[252]	21[258]	GTGCCAAGCTGCAAGTGCGGGGCGCAACTTCTGGTACTCCAGGCCAGTT	49	core92
4[97]	11[104]	AAACAGTTAGACTGTGCAACTAAAGTAAAGCGCAGACGGTCAGAGCTTAA	49	core93
18[69]	23[76]	ATTACCTAGCAAAAAGCGAATTATTCGCTGATTGCAGTAAACAAAAGAAA	49	core94
7[182]	9[174]	ACCCTGAAACATAAAAAACAGGATAAGAAAAGAACAGTAGGGCTGGTTAAG	49	core95
21[154]	18[161]	ATCGCCATGAATGGTCTGGCCAACAGAGAGATTACAGACCTAATAAACAC	49	core96
2[160]	10[154]	TTCATCGTAGGAACGTACCGCATCGGCTATAATATCCCATCCGAATCGC	49	core97
0[237]	8[231]	GTTTTGCAAAAAGAAAACAAAAGAAATATTTACCAGTCACCAATTTTCAT	49	core98
7[203]	11[209]	TAATTTTAGCAGCCTTTACAGAACGTCACCCTTTACCAGAAGGAAACC	49	core99
14[258]	22[252]	AATTCATGCTACAGATAACGTACAGGAGCGCCAGAACCCGTCGGTAATG	49	core100
25[35]	14[28]	TGTTCCAGGACTCCACACAACCGAGCTCGAATTCGGCTTGTTCTCTCTG	49	core101
25[182]	14[175]	TCAATCGCAGAACACATAAAGTGTAATACTTTTGCAAAGGGTTTCTAAT	49	core102
1[252]	7[258]	CGGAACCACAGGAGCTGAATTAAGCCAGTCAGACACCGCCAAGAGCCA	49	core103
2[223]	1[216]	AGTGCCTTGCCCGTCAGGCGGATAAGTGCCGTCGATCTAAGAACAACAG	49	core104
8[230]	7[223]	CGGCATTTCTTTTCGAGCCGCCACCAGAACCACATATTAGCGTTTGCCA	49	core105
22[41]	25[34]	CCCTTACAGTGAGATGAATCGGCCAACGCTTTCCAAATCCCTGAGTGT	49	core106
14[48]	22[42]	TCTCCGAATCACCCAGAACGTGTTTGATTCCGAAAAGGCGAACTGATTG	49	core107
11[245]	0[238]	ATTATTCTACCAGCGCAGTCTGTACTGGTAATAACCCCTGTAGCGGG	49	core108
14[132]	22[126]	GCGGCCACGGGGAGTTGAGACAACCTCAATACATTAATAGATTGGCAA	49	core109
21[217]	18[224]	ATTTTTGTCATTTTCAGCTTTTCATCAACATCAGTGTGTCAATATCAGGT	49	core110
1[63]	7[69]	AATGCAGAGATTTAAACTAACAAGAAAAATGCGATAACTTTAAATAAGG	49	core111
27[182]	18[189]	GCGCTAGACCCCGCGAGAAAAGGCCGAGATGACCCTAAATCAGGTGAT	49	core112
25[119]	14[112]	CAATTCGTAACATTACATCCATCAATAGTGAATTTTAAGACTGTAAGC	49	core113
14[90]	22[84]	ATAGGGGACTAAATGAAGGAGATCCTGAGTTAGAAGATTTTCTCAGATG	49	core114
12[104]	6[98]	TTAAATAGATAGCGTCCAATACCCTCAACATAAATATCAAAAAGATTAG	49	core115
8[41]	11[34]	GGAGTTATATATTCTTCTTAAACAGCTTTAATTGTAACGAGGTTCCATT	49	core116
9[161]	6[154]	GACAAAATAATTGATAATTTACGAGCAAGAAGCGCATTAGTTTATCAAC	49	core117
21[112]	18[119]	AAACCCTGTTGAAAGGAGCACTAACAACCTGAGGAGAGAAAATAGTAGC	49	core118
2[55]	13[62]	CAGTTTTGTCGTCTATAGAAAAGGAACAATGTGTCGGACCCCGAGCGATT	49	core119
0[258]	8[251]	AGAAGGACGGAATATATGGTTATTAAGTGGGAATGCAGCACTTAGCGTC	50	core120
11[140]	2[140]	ATGCGTTTAGCTATAAACCAACAAAATA AAAAAAAAAA	28	handle A10 1
18[160]	27[160]	CGGAATCAGCAAAAACAGGAAAAGGAAG AAAAAAAAAA	28	handle A10 2
20[97]	25[97]	CTAAAGCAAGAAAATGGAAGTTGTTG AAAAAAAAAA	28	handle A10 3
3[77]	4[77]	CATTATTACAGGTTTCTACCAGTCAGGA AAAAAAAAAA	28	handle A10 4
4[181]	2[182]	TCCCAATGAAGCCTTAAATCACGACTTG AAAAAAAAAA	28	handle A10 5
9[140]	4[140]	AATAAGAAACAACGAAGAAAAGTCTTTC AAAAAAAAAA	28	handle A10 6
20[76]	25[76]	CGCAGAGGAAGATGTATCAAAAATTCAT AAAAAAAAAA	28	handle A10 7
18[202]	27[202]	AAACAAGGGTTGTATTGCTGGGCAAGTG AAAAAAAAAA	28	handle A10 8
18[223]	27[223]	CATTGCCCGGAGAGGAAGAACCGGTAA AAAAAAAAAA	28	handle A10 9
11[224]	2[224]	GGAAGGTGGCGACAATCCTGACGGGGTC AAAAAAAAAA	28	handle A10 10

18[48]	25[55]	AAAGTGTAACCTGTCGTGAAATGGTGGACAAGAG AAAAAAAAAA	35	handle A10 11
16[132]	27[139]	ACCCTAGATAAATCATAACAGGTTTAAAAAAGCCGG AAAAAAAAAA	35	handle A10 12
9[91]	4[98]	TAGAGAGTACCTTTGGATGGCGAATGACATGCTTT AAAAAAAAAA	35	handle A10 13
13[210]	2[203]	TACATAAGAAAACGCAATAATATTTGCACGAGGCGT AAAAAAAAAA	35	handle A10 14
18[83]	27[76]	ACAATTTTCATTTGACAATATAATCATCAAGGTGCC AAAAAAAAAA	35	handle A10 15
11[210]	4[203]	GAGGATTTTATCTTACCGAAGAAAATGAGTTACAA AAAAAAAAAA	35	handle A10 16
20[188]	25[181]	AATTGAGCAGAAGAGGTTTGATTATTATTGACGC AAAAAAAAAA	35	handle A10 17
13[126]	2[119]	CAATTCTTTTGGGGCGCGATGATCGTCACAAAAGA AAAAAAAAAA	35	handle A10 18
14[195]	25[202]	CAAAATAGGCGCTGTAATATCTCAAATTAACCGTT AAAAAAAAAA	35	handle A10 19
18[188]	27[181]	AAATAAGGCGTTAACTCAGAGATATTACGGAGCGG AAAAAAAAAA	35	handle A10 20
14[111]	25[118]	AACTCGTGAGCCCTGCGGAACTAGACTTTACAAA AAAAAAAAAA	35	handle A10 21
16[48]	27[55]	CGGGTACATACGAGCCGAGACTATTAATAATCAA AAAAAAAAAA	35	handle A10 22
9[175]	4[182]	CCCAATAATAAGAGAGTAAGCACGATTTTATTTA AAAAAAAAAA	35	handle A10 23
21[140]	25[139]	GATAGCCACACCGCTGCAACAAATATAAATAGATGTATTAA AAAAAAAAAA	42	handle A10 24
10[55]	2[56]	AGATGAACCGCGACCTGCTCCGATAAATTAACGGGAATAC AAAAAAAAAA	42	handle A10 25
13[98]	2[98]	AGTTTCATCAGAGCCATAGTAAGAGCAACCAGAGGGGTAAT AAAAAAAAAA	42	handle A10 26
4[55]	4[56]	TTAACTAAAGGAATTATCAGCTTGCTAATTACCTTATCTACG AAAAAAAAAA	42	handle A10 27
11[161]	4[161]	CAGTATAGCAAATGGAGAACAAGCAATCCATGTAGAAACCA AAAAAAAAAA	42	handle A10 28
21[224]	25[223]	TTAAAGGGAAAAGCCCCAAAACTAGCAAGGCCACTTGATTA AAAAAAAAAA	42	handle A10 29
13[77]	2[77]	ACAAAGTTCAGGGAACGCCAAAAGGAATTGTAGAAAGATTCA AAAAAAAAAA	42	handle A10 30
13[161]	2[161]	AGATACATCACCGTCCCAATAGCAAGCATTGCCGTTTTTATT AAAAAAAAAA	42	handle A10 31
8[223]	4[224]	TTCGGTCCAAGGCCGAAACGTAGCACCCGCCAGCTTCCAG AAAAAAAAAA	42	handle A10 32
18[118]	27[97]	ATATGCTGATGCAAATCCAAAATTAATTAGGTTGGACCACCACGGAACC AAAAAAAAAA	49	handle A10 33
8[125]	4[119]	CTTCAAATTCAAAATGCAAAGCGGATTGCCAAAAATCAGGTCTTATTCAT AAAAAAAAAA	49	handle A10 34
22[167]	25[160]	ATATTTTTTAAAAAGAGGTGAGGCGGTATCTTCTCCAGTCAGTCATG AAAAAAAAAA	49	handle A10 35
25[98]	27[118]	GATTATACAAAGAAGTTATATAACTATATGTAATAATCATTTGATTTA AAAAAAAAAA	49	handle A10 36
8[199]	8[198]	ATATCAATGAAATAGCAATAGCTAGATAGCCCCGAGCGCTA tt TAGCAGCATCACAGATCACA GTATAAAAC CATGACTACCTATCCTACA		Design 1 inverted a
15[210]	15[199]	ATCAATACCGTTCTAGCTGAAAAACATTACAG tt TGTAGGATAGGTAGTCATG GTTTTATAC TGTGATCTGTGATGCTGCTA		Design 1 inverted b
8[199]	8[198]	ATATCAATGAAATAGCAATAGCTAGATAGCCCCGAGCGCTA tt TAGCAGCATCACAGATCACA CTATAAAAG CATGACTACCTATCCTACA		Design 1 consensus a
15[210]	15[199]	ATCAATACCGTTCTAGCTGAAAAACATTACAG tt TGTAGGATAGGTAGTCATG CTTTTATAG TGTGATCTGTGATGCTGCTA		Design 1 consensus b
8[199]	8[198]	ATATCAATGAAATAGCAATAGCTAGATAGCCCCGAGCGCTA tt TAGCAGCATCACAGATCACA ACTTCTCGG CATGACTACCTATCCTACA		Design 1 scramble a
15[210]	15[199]	ATCAATACCGTTCTAGCTGAAAAACATTACAG tt TGTAGGATAGGTAGTCATG CCGAGAAGT TGTGATCTGTGATGCTGCTA		Design 1 scramble b

15[210]	8[200]	ATCAATACCGTTCTAGCTGAAAAACATTACAG tt TAGCAGCATCACAGATCACA GTATAAAAC CATGACTACCTATCCTACA tt ATATCAATGAAATAGCAATAGCTAGATAGCCCCGAGCGCTA		Design 2 a
		TGTAGGATAGGTAGTCATG GTTTTATAC TGTGATCTGTGATGCTGCTA		Design 2 b

Supplementary Table S2: Summary of the angular distribution in various designs and experimental conditions.

Bridge design and sequence	Experimental conditions	Peak position in Histogram	The yield of devices (rounded off)
Design 1 with S1 sequence	Concentration optimization of bridging staples	80±5°	~25%
	• 2-fold excess		~40%
	• 4-fold excess		~37%
	• 6-fold excess		~35%
	• 8-fold excess		~31%
Design 2 with S1 sequence	Concentration optimization of bridging staples	80±5°	~31%
	• 2-fold excess		~37%
	• 4-fold excess		~39%
	• 6-fold excess		~41%
	• 8-fold excess		~39%
Open Devices	Devices with undefined angle	Flat distribution	NA
Design 1 with S1 sequence	Increasing concentrations of TBP		
	• 25 nM TBP	80±5°	~23%
		65±5°	~36%
	• 50 nM TBP	80±5°	~21%
		65±5°	~39%
	• 100 nM TBP	80±5°	~21%
		65±5°	~40%
	• 150 nM TBP	80±5°	~24%
		65±5°	~39%
	Increasing concentration of TBP + TFIIA		
	• 25 nM TBP + 25 nM TFIIA	80±5°	~24%
		55±5°	~34%
	• 50 nM TBP + 50 nM TFIIA	80±5°	~23%
		55±5°	~36%
	• 100 nM TBP + 100 nM TFIIA	80±5°	~16%
		55±5°	~41%
	Constant TBP concentration (50 nM) and increasing concentrations of TFIIA		
	• 50 nM TBP + 0 nM TFIIA	80±5°	~21%
		65±5°	~39%
	• 50 nM TBP + 25 nM TFIIA	80±5°	~23%
	No second peak	NA	
• 50 nM TBP + 50 nM TFIIA	80±5°	~24%	
	55±5°	~34%	
• 50 nM TBP + 100 nM TFIIA	80±5°	~19%	
	55±5°	~36%	

	Increasing concentration of TBP + TFIIB		
	• 25 nM TBP + 25 nM TFIIB	80±5°	~23%
		65±5°	~29%
	• 50 nM TBP + 50 nM TFIIB	80±5°	~22%
		65±5°	~38%
	• 100 nM TBP + 100 nM TFIIB	80±5°	~18%
		65±5°	~40%
	Increasing concentration of TBP + TFIIA+ TFIIB		
	• 25 nM TBP + 25 nM TFIIA + 25 nM TFIIB	80±5°	~23%
		55±5°	~27%
	• 50 nM TBP + 50 nM TFIIA + 50 nM TFIIB	80±5°	~24%
		55±5°	~31%
	• 100 nM TBP + 100 nM TFIIA + 100 nM TFIIB	80±5°	~20%
		55±5°	~37%
	Control experiments		
• 50 nM TFIIA	80±5°	~43%	
• 50 nM TFIIB	80±5°	~38%	
Design 1 with S2 sequence	Increasing concentrations of TBP		
	• 25 nM TBP	80±5°	~28%
		65±5°	~25%
	• 50 nM TBP	80±5°	~27%
		65±5°	~30%
	• 100 nM TBP	80±5°	~24%
		65±5°	~31%
	Increasing concentration of TBP + TFIIA		
	• 25 nM TBP + 25 nM TFIIA	80±5°	~23%
		55±5°	~33%
	• 50 nM TBP + 50 nM TFIIA	80±5°	~22%
55±5°		~37%	
• 100 nM TBP + 100 nM TFIIA	80±5°	~19%	
	55±5°	~39%	
Design 1 with S3 sequence	Control devices forming an 80° angle between the bundles	80±5°	~41%
	Control devices incubated with		
	• 50 nM TBP	80±5°	~40%
	• 50 nM TBP + 50 nM TFIIA	80±5°	~41%
	• 50 nM TBP + 50 nM TFIIB	80±5°	~39%

References

- 1 J. L. Kim, D. B. Nikolov and S. K. Burley, *Nature*, 1993, 365, 520–527.
- 2 Y. Kim, J. H. Geiger, S. Hahn and P. B. Sigler, *Nature*, 1993, 365, 512–520.
- 3 P. F. Kosa, G. Ghosh, B. S. DeDecker and P. B. Sigler, *PNAS*, 1997, 94, 6042–6047.